

*Received November 5, 2016; reviewed; accepted April 4, 2017*

## **Behavior of gallium and germanium associated with zinc sulfide concentrate in oxygen pressure leaching**

**Fupeng Liu<sup>\*</sup>, Zhihong Liu<sup>\*</sup>, Yuhu Li<sup>\*</sup>, Benjamin P. Wilson<sup>\*\*</sup>, Mari Lundstrom<sup>\*\*</sup>**

<sup>\*</sup> School of Metallurgy and Environment, Central South University, Changsha 410083, China. Corresponding author: Fupengliu@126.com (Fupeng Liu)

<sup>\*\*</sup> Department of Materials Science and Engineering, Aalto University, School of Chemical Technology, Vuorimiehentie 2, 02150 Espoo, Finland

**Abstract:** The Fankou zinc concentrate (Guangdong province, China) was mineralogically characterized and results showed that the main germanium-bearing minerals in the sample comprised of zinc sulfide and galena, whereas gallium-bearing minerals were pyrite, sphalerite and silicate. Oxygen pressure leaching of zinc sulfide concentrate was carried out in order to investigate the effect of pressure, leaching time, sulfuric acid and copper concentrations on the leaching behavior of gallium and germanium. Under optimum conditions, leaching of Zn, Fe, Ge and Ga reached 98.21, 90.45, 97.45 and 96.65%, respectively. In the leach residues, it was determined that some new precipitates, such as PbSO<sub>4</sub>, CaSO<sub>4</sub> and SiO<sub>2</sub>, were formed, which co-precipitated a certain amount of Ga and Ge from the leach solution. The results clearly indicated that Ga and Ge were much more difficult to leach than Zn, and provided answers to why the leaching efficiency of Ga is 10% lower when compared to Ge.

**Keywords:** *zinc sulfide concentrate, gallium, germanium, pyrite, oxygen pressure leaching*

### **Introduction**

Gallium and germanium are critical materials that play important roles in high-technology fields like liquid crystal displays, semiconductors, infrared optics etc. (Schimmel et al., 2001; Wan et al., 2002; Depuydt et al., 2006; Tyszczyk et al., 2007). Until now, no commercially viable independent ore deposits of Ga and Ge have been found in the nature, thus as a result, these scarce metals are generally recovered as by-products from metallurgical processes of other nonferrous metals, like zinc, lead and aluminum. In addition, coal fly ash has also been identified as another promising secondary source for Ga and Ge (Torrvalvo et al., 2011). In China, zinc sulfide concentrates produced from some mining areas, especially those located in either south or southwest China, such as the Dachang mine in the Guangxi province, Fankou

mine in the Guangdong province and Huize mine in the Yunnan province, are particularly rich in Ga and Ge. Ga and Ge are able to replace zinc and other metals within the crystal lattice structure of sphalerite, by far the most important economic source of Ga and Ge, thus, these metals are often associated with zinc sulfides. Nevertheless, concentrations of Ga and Ge in different deposit types show a great deal of variation as a result of elemental fractionation into sphalerite, which is influenced by the crystallization temperature, metal source and sphalerite content in the ore (Cook et al., 2009, 2015; Ye et al., 2011; Frenzel et al., 2014, 2016). Currently, in the traditional roast-leach-electrowinning process of zinc hydrometallurgy, Ga and Ge can only be retrieved from these zinc sulfide concentrates with low rates of recovery and significantly high costs.

Development of oxygen pressure leaching provides a more efficient way to extract germanium and gallium from a zinc sulfide concentrate. Studies on oxygen pressure leaching of zinc sulfide concentrate began in the 1950s and have continued for more than 60 years, leading to hundreds of associated published papers (Collins et al., 1994; Jankola et al., 1995; Krysa et al., 1995; Ozberk et al., 1995). These studies have investigated a wide range of aspects including: thermodynamics and kinetics of leaching (Baldwin et al., 1995; Rubisov et al., 1995; Tromans, 1998; Markus et al., 2004; Lampinen et al., 2015), oxygen solubility modeling in acidic zinc sulfate solutions (Kaskiala, 2002), effects of additives and their mechanisms (Owusu et al., 1995; Tong et al., 2009a), leaching behavior of silver and indium in oxygen pressure leaching (Bolorunduro et al., 2003; Li et al., 2010; Cook et al., 2011), recovery of elemental sulfur from the leaching residues (Brown et al., 2005; Tong et al., 2009b; Halfyard et al., 2011). The commercial use of oxygen pressure leaching of zinc sulfide concentrate began in the early 1980's and is currently in use in Canada, Germany and China (Ozberk et al., 1995; Zuo, 2009).

In China, the first zinc hydrometallurgical plant to use oxygen pressure leaching – the Danxia smelter, North Guangdong province – was commissioned in 2011 and now produces approximately 120,000 Mg of zinc ingots annually. The zinc sulfide concentrate treated by the Danxia smelter, contains from 0.01 to 0.02 wt% Ga/Ge and is specially supplied by the nearby Fankou mine. The prime motivation for utilizing oxygen pressure leaching at the Danxia smelter is to recover the associated Ga and Ge from the Fankou zinc sulfide concentrate during the zinc hydrometallurgical process (Zuo, 2009). In the two-stage counter current leaching process, more than 98% of zinc is leached from the concentrate, whereas the associated leaching efficiencies for Ga and Ge are only about 70% and 80%, respectively. Until now the reasons for the fact that Ga and Ge are more difficult to be leached than zinc, as well as why the leaching efficiency of Ga is 10% lower than that of Ge, have been unknown. In order to determine these observations, the behavior of Ga and Ge under oxygen pressure leaching conditions were investigated using the Fankou zinc sulfide concentrate as the raw material.

## Material and methods

### Material characterization

The Fankou zinc concentrate used in this study was supplied by the Danxia smelter. Prior to the leaching experiments, approximately 10 kg of concentrate was ground in a laboratory ball mill to achieve the grain size distribution. The chemical composition and the particle size of the zinc concentrate are shown in Table 1 and 2, respectively. As can be seen in Table 1, the contents of gallium and germanium in the zinc concentrate were determined to be 0.0130 and 0.0168 wt%, respectively.

Table 1. Chemical composition of the concentrate used in leaching experiments (wt %)

Zn	Fe	S	Mn	Cu	Pb	As	Ga	Ge	SiO <sub>2</sub>
53.00	6.40	33.70	0.03	0.11	0.94	0.98	0.0130	0.0168	2.68

The particle size of the sample (Table 2) was done by a wet screen analysis, which showed that near 80 wt % of the particles in the zinc concentrate was < 38  $\mu\text{m}$ . In addition, the composition of iron phase was also obtained through a chemical analysis method and is shown in Table 3. Moreover, the analysis showed that the iron content in the zinc concentrate was only 6.40 wt % with pyrite forming the main phase (63.43 wt %).

Table 2. Particle size distribution of the Fankou zinc concentrate

Particle size, $\mu\text{m}$	<38	38~48	54~74	>74
Distribution, wt %	79.56	16.58	2.58	1.28

Table 3. Iron phases in the Fankou zinc concentrate

Iron phases	Pyrrhotite	Pyrite	Siderite	Hematite	Magnetite	Iron silicate	$\Sigma\text{Fe}$
Mass fraction (wt%)	0.66	4.06	0.18	0.97	0.03	0.50	6.40
Distribution (wt%)	10.31	63.43	2.81	15.15	0.46	7.81	100

In order to better simulate the conditions found during smelter production, a feedstock comprising of a synthetic aqueous solution containing 60  $\text{g}/\text{dm}^3$   $\text{Zn}^{2+}$ , 3  $\text{g}/\text{dm}^3$   $\text{Fe}^{2+}$ , 0.5  $\text{g}/\text{dm}^3$  sodium lignosulfonate and 3  $\text{g}/\text{dm}^3$   $\text{Mn}^{2+}$  was prepared. Analytical grade reagents of sulfuric acid, ferrous sulfate, copper sulfate, sodium lignosulfonate were used without any further purification and deionized water was used in the experiments.

The crystal phases present within the samples were identified by a Rigaki-TTRIII X-ray diffractometer (Cu target,  $\text{K}\alpha_1$ ,  $\lambda = 0.15406$  nm). The microstructure and phase composition of the sample was initially examined using a JSM-6306 Scanning Electron Microscope (SEM) with an EDX-GENESIS 60S Energy Dispersive

Spectrometer (EDS). In addition, samples were also measured using an Electron-Probe X-ray Microanalysis (EPMA) performed with a JEOL JXA-8230 instrument equipped with five wavelength dispersive X-ray spectrometers (WDS). An accelerating voltage of 20 kV, beam current of 10 nA and beam diameter between 1 to 5  $\mu\text{m}$  were utilized in the analysis. The standards of Ga and Ge used in this work were artificial compound (GaAs for Ga,  $L\alpha$ ; GeS for Ge,  $L\alpha$ ). Silica concentration in the leach solutions was determined using the silicon molybdenum blue spectrophotometry method. Zinc concentration in the leach solutions was analyzed by EDTA titration, whereas the concentrations of Ga, Fe and Cu in the leach residues or solutions were determined using a Thermo Electron IRIS Interpid II XSP ICP-AES spectrometer. The germanium concentration in the leach residue or solutions was found using the extraction separation-benzfluorenone spectrophotometry method.

### **Oxygen pressure leaching procedure**

Synthetic aqueous solutions that contained zinc, manganese, sulfuric acid, ferrous sulfate and sodium ligninsulfonate were used as the leach solutions. The pressure acid leaching test was performed by mixing the zinc sulfide concentrate and synthetic aqueous solutions at a predetermined liquid-to-solid ratio (L/S) and 600 rpm in a 2  $\text{dm}^3$ , PTFE lined, vertical autoclave (GSHA-2, Weihai Weihua Chemical Machinery Instrument Co., China). After the autoclave was heated to the set temperature (159 °C) for a certain time at a desired pressure, the heating was stopped, and the autoclave naturally cooled to room temperature. After filtration, leach residues were washed with deionized water and both the residue and filtrate samples were analyzed. Leaching temperature was set at 159 °C as the viscosity of the molten elemental sulfur was minimum between 119 (melting point of sulfur) and 200 °C (Meyer, 1976; Owusu, 1985). This low viscosity helps to prevent occlusion of molten elemental sulfur to the zinc concentrate, which, in turn, aids diffusion of dissolved oxygen to the mineral surface and the subsequent oxidation reaction.

## **Results and discussion**

### **States of gallium and germanium in Fankou zinc sulfide concentrate**

The XRD pattern of the Fankou zinc sulfide concentrate, shown in Fig. 1, demonstrates that the concentrate comprises primarily of minerals like sphalerite (85.2%), pyrite (9.0%), galena (1.2%) and quartz (2.6%). The Electron-Probe X-ray Microanalysis (EPMA) quantitative analysis of the same concentrate was performed in order to ascertain the associated chemical states of gallium and germanium. Figure 2 displays the back scattered electron image that was investigated using 20 separately located analysis points located in 19 individual mineral particles (points 7 and 8 were located in the same mineral particle). From the results outlined in Table 4, it was possible to determine the minerals present in the zinc concentrate.

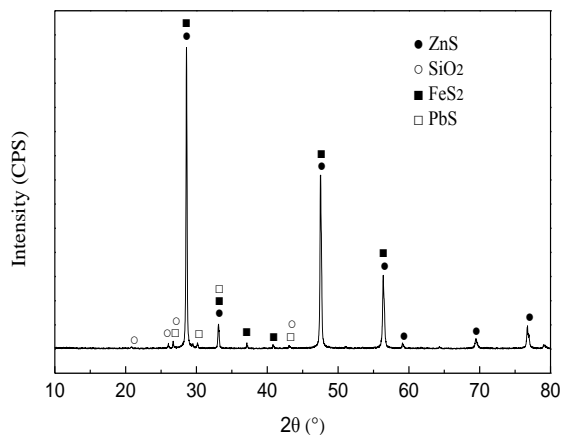


Fig. 1. XRD pattern of the Fankou zinc sulfide concentrate

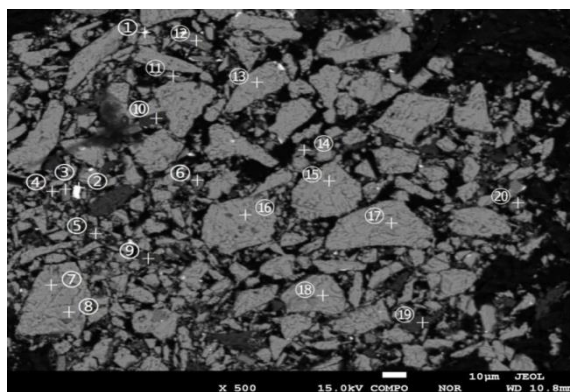


Fig. 2. Backscattered electron image of the Fankou zinc sulfide concentrate

From the data shown in Fig. 2 and Table 4, it was possible to resolve the presence of the following minerals: particles 1 and 2, with a white coloration were galena; particles 3 to 6, 11, 12, 14 and 20, that had a dark grey color, were pyrite; particles 7, 13, 15 to 18 (light grey color) were sphalerite; finally, particles 9, 10 and 19 with the charcoal grey color were found to be quartz with small amounts of silicate (aluminium silicate, iron silicate). Furthermore, this analysis suggested that there were no independent gallium or germanium minerals present in the concentrate. When comparing to Table 4, it provides that gallium was incorporated mainly within minerals like quartz with small amounts of silicate, pyrite and sphalerite, whereas germanium was found primarily in conjunction with sphalerite and galena. It is also clear that Ga and Ge were preferentially enriched in sphalerite relative to other sulfides, which is in line with previous observations by George et al. (2016). These findings indicate that the behavior of zinc, gallium and germanium can be different during oxygen pressure leaching of the Fankou zinc sulfide concentrate.

In order to better understand the behavior of gallium and germanium associated with the Fankou zinc sulfide concentrate during oxygen pressure leaching, the effects of oxygen pressure, leaching time and the concentrations of sulfuric acid and  $\text{Cu}^{2+}$  ions on Zn, Fe, Ge, Ga leaching were investigated.

Table 4. EPMA results of the spots shown in Fig. 2 (wt %)

Spot	Mineral	O	Si	Ge	S	Ga	Zn	Fe	Pb	Cu	Al	Ca	Total
1	Galena	0.215	ND	0.026	11.6	ND	4.51	0.671	81.4	0.140	0.160	ND	98.6
2	Galena	0.587	0.074	ND	11.55	ND	4.50	0.460	82.23	ND	0.022	0.03	99.5
3	Pyrite	0.583	ND	ND	52.9	0.036	1.52	44.4	0.294	0.035	0.011	ND	99.8
4	Pyrite	1.96	2.00	ND	50.0	0.019	2.21	43.0	0.331	ND	ND	ND	99.5
5	Pyrite	1.70	0.153	ND	51.2	0.021	2.08	43.2	0.279	0.059	0.031	ND	98.7
6	Pyrite	0.913	0.223	ND	52.26	0.017	2.59	43.7	0.118	0.025	0.103	0.021	99.8
7	Sphalerite	0.217	0.044	0.039	34.4	0.020	63.1	2.20	0.028	ND	ND	ND	100
8	Sphalerite	0.989	0.021	0.018	33.9	0.022	63.6	1.49	0.054	0.027	0.026	ND	99.9
9	Quartz	53.7	39.7	ND	1.62	0.018	2.38	0.983	0.072	0.016	0.838	0.034	99.5
10	Quartz	50.5	43.0	ND	0.294	0.043	1.07	0.101	1.85	ND	2.731	0.025	99.6
11	Pyrite	1.37	ND	0.024	49.4	ND	5.79	40.7	0.057	0.039	0.651	0.042	98.3
12	Pyrite	0.488	0.205	ND	54.6	0.019	0.128	43.2	0.188	ND	ND	0.132	99.0
13	Sphalerite	0.765	0.054	0.035	33.9	0.046	64.3	1.33	0.145	0.100	ND	ND	100
14	Pyrite	4.86	1.75	ND	49.7	0.019	2.04	42.0	0.064	0.058	ND	ND	100
15	Sphalerite	0.465	0.032	0.019	34.5	0.023	63.8	1.16	0.077	0.134	0.132	ND	99.7
16	Sphalerite	0.365	0.041	0.021	33.9	ND	63.1	0.73	0.017	0.092	0.054	0.016	99.0
17	Sphalerite	0.765	0.124	0.025	34.9	0.021	62.2	1.58	0.215	0.122	ND	ND	100
18	Sphalerite	0.122	0.101	0.018	33.5	ND	65.8	0.145	0.028	0.132	ND	ND	100
19	Quartz	52.4	44.1	ND	0.146	0.023	1.12	0.401	0.249	ND	1.231	ND	99.6
20	Pyrite	0.165	ND	ND	52.1	0.026	2.84	45.0	0.055	0.024	ND	ND	100

ND – not detected at a minimum detection limit of 100 ppm

### Effect of oxygen pressure

As can be seen in Fig. 3, the level of oxygen pressure has a significant influence on leaching of Zn, Fe, Ge and Ga. With an increase of oxygen pressure from 0.4 to 1.2 MPa, the leaching efficiencies of Zn, Fe, Ge and Ga are observed to increase from 79.31 to 97.13, 58.60 to 75.79, 68.70 to 90.15 and 60.56 to 87.65%, respectively. Furthermore, there is a clear systematic difference in the overall leaching efficiency, with the sequence, from high to low, being Zn, Ge, Ga and Fe. These results are consistent with those achieved during industrial production at the Danxia smelter, which also has the highest extraction rates for Zn and the lowest for Fe.

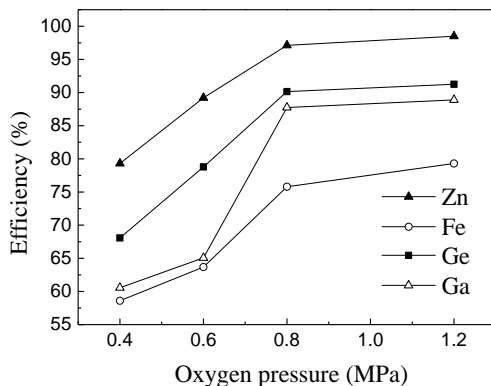


Fig. 3. Effect of oxygen partial pressure on the leaching efficiency of the Zn, Fe, Ge, Ga ( $[\text{H}_2\text{SO}_4] = 180 \text{ g/dm}^3$ ,  $t = 2 \text{ h}$ ,  $T = 159 \text{ }^\circ\text{C}$ ,  $L/S = 8 \text{ cm}^3/\text{g}$ )

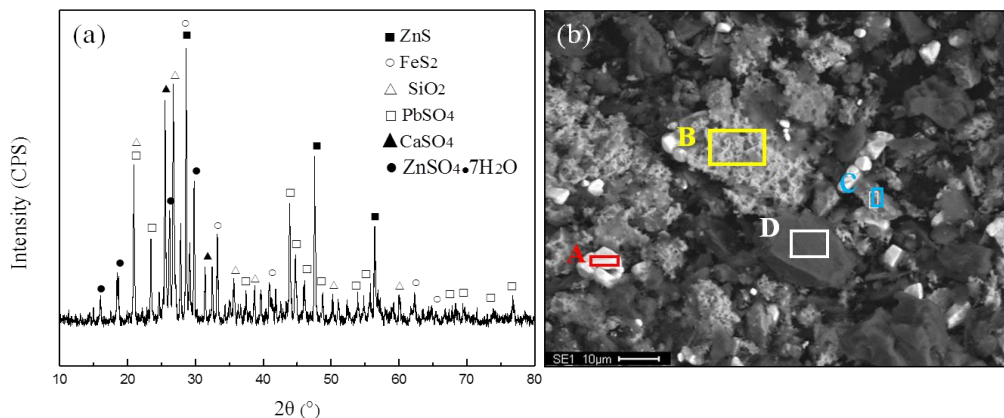


Fig. 4. XRD pattern (a) and EDS image (b) of leaching residues after removing elemental sulfur by washing with  $\text{CS}_2$  ( $p(\text{O}_2) = 0.8 \text{ MPa}$ ,  $[\text{H}_2\text{SO}_4] = 180 \text{ g/dm}^3$ ,  $t = 2 \text{ h}$ ,  $T = 159 \text{ }^\circ\text{C}$ ,  $L/S = 8 \text{ cm}^3/\text{g}$ )

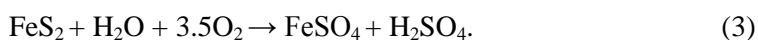
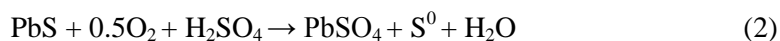
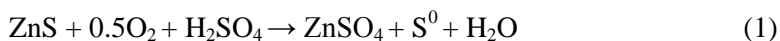
Table 5. EDS results of the leaching residues in Fig. 4b (atom fraction %)

Analysis	Zn	Fe	Pb	S	Si	O	Ga	Ge
A	1.03	0.00	37.7	34.3	1.25	25.7	0.00	0.00
B	43.1	1.68	0.00	49.0	6.31	0.00	0.00	0.00
C	1.89	32.3	0.00	62.2	3.60	0.00	0.13	0.00
D	0.00	0.00	0.00	2.25	32.5	65.5	0.02	0.01

The leaching obtained at an oxygen pressure of 0.8 MPa (elemental sulfur produced in leaching was washed out using  $\text{CS}_2$ ) were analyzed by XRD and SEM-EDS, respectively. The results, shown separately in Figs. 4a and 4b as well as Table 5,

demonstrate that with the exception of elemental sulfur, the main phases in the leach residue were pyrite, sphalerite, quartz and sulfates of lead and calcium.

The main reason suggested for the observed differences in the leaching efficiency of Zn, Fe, Ge and Ga is the variation of minerals to which the metals are associated. Sphalerite and galena are known to be relatively easy to leach when compared to the pyrite or quartz and the main reactions are:



As a result, pyrite and quartz remain in the leach residue in high proportions, resulting in the lower leaching efficiencies measured for the associated Fe, Ga and Ge when compared to Zn. This correlates with the previous observations of Papangelakis and Demopoulos (1991). They showed that only 70% of pyrite dissolution occurred with an oxygen pressure of 1.013 MPa at 150 °C for 2 h, which suggested that pyrite was relatively difficult to leach within the system under investigation. More in depth analysis of the Ga and Ge states, present in the concentrate, showed that pyrite and silica contained more Ga than Ge. This in turn, leads to the observed lower leaching efficiency for Ga when compared to that of Ge.

### Effect of leaching time

The effect of leaching time on separation of Zn, Fe, Ge, Ga is shown in Fig. 5. It can be seen that over 97% of Zn, 90% of Ge and almost 88% of Ga was leached out after 2 h. Moreover, it was observed that further increase in the leaching time had little influence on the concentration of Zn, Fe, Ge and Ga in the leaching solution. Figure 5 shows that the Ge leaching curve is similar to Zn leaching curve, in contrast, the Ga curve is more analogous to Fe. This suggests that Ge leaching is dominated by the leaching behavior of sphalerite, whereas Ga leaching is more affected by the kinetics of pyrite dissolution. Tables 3 and 4 show that pyrite in both the Fankou zinc sulfide concentrate and in the leach residues contained some Zn and Ga resulting in a lower leaching recovery. In addition, extraction of gallium from the concentrate was found to be both constantly inferior to that of germanium and to decrease after 2 h of leaching. These findings suggest that the leaching time should be limited to 2 h as this would require lower energy consumption as well as increase the plant productivity.

### Effect of sulfuric acid concentration

Figure 6 shows the effects of sulfuric acid concentration on leaching of Zn, Fe, Ge and Ga. As it can be seen, with the increase in the initial sulfuric acid concentration from 60 g/dm<sup>3</sup> to 200 g/dm<sup>3</sup>, the recovery of Zn, Fe, Ge and Ga increased but still showed distinct differences. Leaching of Zn and Ge increased slowly at an almost identical



rate as the sulfuric acid concentration increased from 100 g/dm<sup>3</sup> to 180 g/dm<sup>3</sup> (90.24 to 97.13% and 81.80 to 90.15%, respectively) and also the recovery of Zn was higher than Ge. The overall differences between these two elements also remained constant, as the level of Zn leaching was systematically higher than Ge. In contrast, the leaching efficiencies of Ga and Fe had almost identical shapes of leaching curves as the curve of initial sulfuric acid concentration and there was a noticeably sharp increase above [H<sub>2</sub>SO<sub>4</sub>] = 80 g/dm<sup>3</sup>. The recovery of Ga and Fe increased from 40.58 to 87.65% and 50.55 to 75.59%, respectively, with increasing sulfuric acid concentration from 100 g/dm<sup>3</sup> to 180 g/dm<sup>3</sup>. Such observations can be attributed to the differences in the occurrence states between Ge and Ga in the Fankou zinc sulfide concentrate.

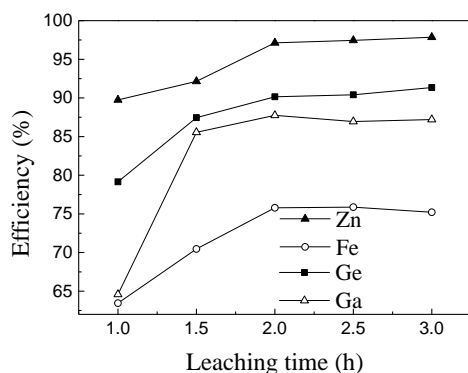


Fig. 5. Effect of leaching time on the leaching of Zn, Fe, Ge, Ga ( $p(\text{O}_2) = 0.8 \text{ MPa}$ ,  $[\text{H}_2\text{SO}_4] = 180 \text{ g/dm}^3$ ,  $T = 159 \text{ }^\circ\text{C}$ ,  $L/S = 8 \text{ cm}^3/\text{g}$ )

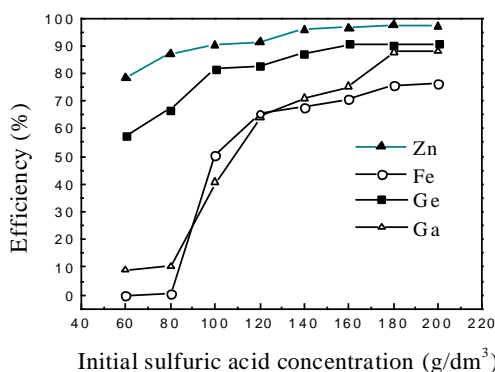
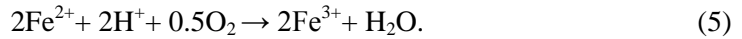
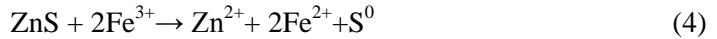


Fig. 6. Effect of sulfuric acid concentration on the leaching of Zn, Fe, Ge, Ga ( $p(\text{O}_2) = 0.8 \text{ MPa}$ ,  $t = 2 \text{ h}$ ,  $T = 159 \text{ }^\circ\text{C}$ ,  $L/S = 8 \text{ cm}^3/\text{g}$ )

From the results shown in Figure 6, it can also be concluded that the increase in sulfuric acid concentration can accelerate leaching of pyrite more dramatically, when compared to the corresponding the leaching of Ga. The increase in acidity does also

accelerate leaching of metallic sulfides which results from the enhanced oxidation reaction of Fe(II) to Fe(III). The net reactions for leaching of zinc sulfide concentrate are:



When the initial acidity is lower than  $100 \text{ g/dm}^3$ , jarosite was formed (as shown in Fig. 7) leading to a loss of germanium (Liang et al., 2009). Although an increase in sulfuric acid concentration is desirable for zinc concentrate leaching, the recovery of Zn, Fe, Ge and Ga only slightly increases when the sulfuric acid concentration changes from  $180$  to  $200 \text{ g/dm}^3$ . Thus, the most suitable concentration of sulfuric acid in the process was selected to be  $180 \text{ g/dm}^3$ .

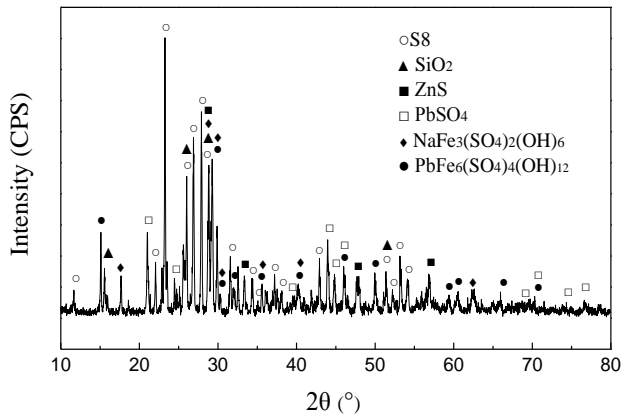


Fig. 7. XRD pattern of leach residue ( $p(\text{O}_2) = 0.8 \text{ MPa}$ ,  $[\text{H}_2\text{SO}_4] = 80 \text{ g/dm}^3$ ,  $t = 2 \text{ h}$ ,  $T = 159 \text{ }^\circ\text{C}$ ,  $L/S = 8 \text{ cm}^3/\text{g}$ )

### Effect of $\text{Cu}^{2+}$ concentration

The effect of  $\text{Cu}^{2+}$  on leaching of the zinc concentrate was also studied and the results are presented in Fig. 8. The extraction of Zn, Ga and Ge significantly increased with increased concentrations of  $\text{Cu}^{2+}$ , for example, for  $0.3 \text{ g/dm}^3 \text{ Cu}^{2+}$ , 97.45% of Ge and 96.65% of Ga were leached out within 120 min, and leaching of Zn and Fe reached 98.21 and 90.45%, respectively. In contrast, further increase in  $\text{Cu}^{2+}$  concentration above  $0.3 \text{ g/dm}^3$  had limited impact on leaching of Zn, Ge, Fe and Ga. It was probably due to the fact that the presence of  $\text{Cu}^{2+}$  could catalyze the oxidation reaction between  $\text{Fe}^{2+}$  and  $\text{O}_2$ . According to the empirical expression (Baldwin et al., 1995) for the rate of ferrous oxidation in the zinc pressure leaching system, the rate of oxidation of  $\text{Fe}^{2+}$  by  $\text{O}_2$  in presence of  $0.1 \text{ g/dm}^3 \text{ Cu}^{2+}$  was over 2.5-fold higher when compared to the

same system in the absence of copper. This is mainly attributed to the oxygen transfer function of the dissolved iron within the leach system.

The EMPA quantitative analysis results of the leach residue are shown in Fig. 9 and Table 6. It can be inferred that the main phase in particles 1, 3, 5, 7, 10, 13 were pyrite, which contain a small quantity of gallium which was difficult to be leached out. On the other hand, particles 2, 8, 9, 11, 12, 14, 15 contained minor amounts of both gallium and germanium, present primarily in either the gypsum, silica or lead sulfate phases.

The results revealed that germanium was primarily distributed in minerals like quartz and insoluble sphalerite, whereas gallium was found primarily in conjunction with insoluble pyrite and quartz. In addition, some new precipitates like  $\text{PbSO}_4$ ,  $\text{CaSO}_4$  and  $\text{SiO}_2$  were formed during the leaching process and led to co-precipitation of a certain amount of Ga and Ge from the leach solution.

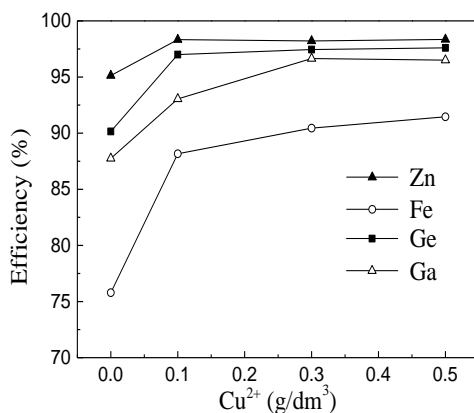


Fig. 8. Effect of  $\text{Cu}^{2+}$  concentration on the leaching of Zn, Fe, Ge, Ga ( $p(\text{O}_2) = 0.8$  MPa,  $[\text{H}_2\text{SO}_4] = 180$  g/dm<sup>3</sup>,  $t = 2$  h,  $T = 159$  °C,  $L/S = 8$  cm<sup>3</sup>/g )

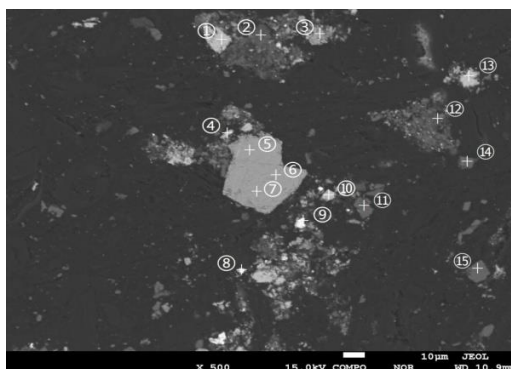


Fig. 9. Backscattered electron image of the leach residues ( $p(\text{O}_2) = 0.8$  MPa,  $[\text{H}_2\text{SO}_4] = 180$  g/dm<sup>3</sup>,  $t = 2$  h,  $T = 159$  °C,  $L/S = 8$  cm<sup>3</sup>/g,  $[\text{Cu}^{2+}] = 0.3$  g/dm<sup>3</sup>)

Table 6. EPMA results of the spots shown in Fig. 9 (wt %)

Spot	Mineral	O	Si	Ge	S	Ga	Zn	Fe	Pb	Ca	Total
1	Pyrite	0.371	0.029	ND	52.3	ND	0.041	45.2	ND	ND	97.9
2	Quartz	50.9	47.1	0.018	0.107	0.019	0.195	0.125	ND	0.041	98.5
3	Pyrite	9.55	6.02	0.011	44.1	0.024	2.78	34.1	ND	0.056	96.9
4	Sphalerite	1.17	ND	ND	33.1	0.011	65.4	2.10	0.231	0.034	99.9
5	Pyrite	1.06	ND	0.016	52.1	0.012	1.39	44.4	0.325	0.031	99.4
6	Pyrite	0.651	0.006	ND	52.6	0.022	0.818	45.3	0.246	ND	99.7
7	Pyrite	0.447	0.011	ND	53.2	0.018	1.05	44.8	0.366	ND	100
8	Anglesite	18.9	0.024	0.014	11.3	0.012	0.624	0.068	65.9	1.46	98.4
9	Anglesite	20.4	0.011	0.010	10.2	ND	0.465	ND	66.1	0.146	97.3
10	Pyrite	0.98	0.012	ND	51.4	0.017	1.23	46.3	0.091	ND	100
11	Quartz	52.8	45.6	0.021	0.107	0.015	0.206	0.421	0.212	0.041	99.4
12	Gypsum	43.0	ND	0.010	13.2	0.023	0.022	ND	0.060	41.0	97.3
13	Pyrite	0.672	ND	ND	52.8	ND	0.243	45.3	ND	ND	99.1
14	Quartz	56.6	39.5	0.015	1.34	0.018	0.145	0.125	ND	1.56	99.3
15	Quartz	54.2	42.7	0.017	0.455	0.015	0.104	0.228	ND	ND	98.0

ND – not detected at a minimum detection limit of 100 ppm

From Table 7 it can be seen that leaching of silicate from the zinc concentrate leads to formation of dissolved silicon in the solution. The presence of this silicon generates silica gel and silica that complexes both Ge and Ga to form both  $\text{SiO}_2 \cdot n\text{H}_2\text{O}$  with 0.008% (Ge) and 0.014% (Ga) and  $\text{SiO}_2$  with 0.016% (Ge) and 0.022% (Ga), which results in lower recovery of Ge and Ga into the solution. The transformation process during leaching is given by reaction:



Table 7. Phase composition of silicon in the zinc concentrate and leach residues by chemical analysis ( $p(\text{O}_2) = 0.8 \text{ MPa}$ ,  $[\text{H}_2\text{SO}_4] = 180 \text{ g/dm}^3$ ,  $t = 120 \text{ min}$ ,  $T = 159 \text{ }^\circ\text{C}$ ,  $L/S = 8 \text{ cm}^3/\text{g}$ ,  $[\text{Cu}^{2+}] = 0.3 \text{ g/dm}^3$ )

Silicon phases	Zinc concentrate			Leaching residues		
	(wt%)	Distribution (%)	(wt %)	Distribution (%)	Ge (wt %)	Ga (wt %)
$\text{SiO}_2$	1.78	66.4	6.29	94.4	0.016	0.022
$\text{SiO}_2 \cdot n\text{H}_2\text{O}$	0.000	0.000	0.210	3.20	0.008	0.014
$\text{MeO} \cdot \text{SiO}_2$	0.900	33.6	0.170	2.40	0.000	0.000
Total	2.68	100	6.67	100	0.024	0.036

## Conclusions

1. In the Fankou zinc concentrate, Ga existed primarily in pyrite, sphalerite and quartz with small amounts of silicate, whereas germanium was found primarily in

conjunction with sphalerite and galena. Moreover, the distributions of Ga and Ge in different particles of the same mineral were non-uniform.

2. The reasons for the low recovery of Ga and Ge are as follows: *i*) the main minerals containing Ga ( $\text{FeS}_2$ ), are more difficult to leach when compared to those containing Ge ( $\text{ZnS}$  and  $\text{PbS}$ ); *ii*) during the leaching process, some new precipitates like  $\text{PbSO}_4$ ,  $\text{CaSO}_4$  and  $\text{SiO}_2$  are formed, which co-precipitate a certain amount of Ga and Ge from the leach solution.
3. The  $\text{Cu}^{2+}$  ions can accelerate leaching, especially of Fe and Ga. Leaching of the Fankou zinc concentrate under the controlled conditions with an addition of  $0.3 \text{ g/dm}^3$   $\text{Cu}^{2+}$  ions, led to increase in the leaching efficiencies of Zn, Fe, Ge, Ga up to 98.21, 90.45, 97.45 and 96.65%, respectively.

### Acknowledgements

This work was financially supported by the National Science Foundation of China (51574285).

### References

- BALDWIN, S.A., DEMOPOULOS, G.P., PAPANGELAKIS, V.G., 1995. *Mathematical modeling of the zinc pressure leach process*, Metall. Mater. Trans. B 26(5), 1035-1047.
- BOLORUNDURO, S.A., DREISINGER, D.B., WEERT, G.V., 2003. *Fundamental study of silver deportment during the pressure oxidation of sulphide ores and concentrates*, Miner. Eng. 16(8), 695-708.
- BROWN, J.A., PAPANGELAKIS, V.G., 2005. *Interfacial studies of liquid sulphur during aqueous pressure oxidation of nickel sulphide*, Miner. Eng. 18(15), 1378-1385.
- COLLINS, M.T., MCCONAGHY, E.J., STAUFFER, R.F., DESROCHES, G.J., KRYSA, B.D., 1994. *Starting up the sherritt zinc pressure leach process at Hudson Bay*, J. Met. 46(4), 51-58.
- COOK, N.J., CIOBANU, C.L., PRING, A., SKINNER, W., DANYUSHEVSKY, L., SHIMIZU, M., SAINI-EIDUKAT, B., MELCHER, F., 2009. *Trace and minor elements in sphalerite: A LA-ICP-MS study*, Geochim. Cosmochim. Acta 73, 4761-4791.
- COOK, N.J., CIOBANU, C.L., WILLIAMS, T., 2011. *The mineralogy and mineral chemistry of indium in sulphide deposits and implications for mineral processing*, Hydrometallurgy 108(108), 226-228.
- COOK, N.J., ETSCHMANN, B., CIOBANU, C.L., GERAKI, K., HOWARD, D., WILLIAMS, T., RAE, N., PRING, A., CHEN, G., JOHANNESSEN, B., BRUGGER, J., 2015. *Distribution and Substitution Mechanism of Ge in a Ge-(Fe)-Bearing Sphalerite*, Minerals 5, 117-132.
- DEPUYDT, B., THEUWIS, A., ROMANDIC, I., 2006. *Germanium: From the first application of Czochralski crystal growth to large diameter dislocation-free wafers*, Mater. Sci. Semicond. Process. 9(4), 437-443.
- FRENZEL, M., KETRIS, M.P., GUTZMER, J., 2014. *On the geological availability of germanium*, Mineralium Deposita 49, 471-486.
- FRENZEL, M., HIRSCH, T., GUTZMER, J., 2016. *Gallium, germanium, indium, and other trace and minor elements in sphalerite as a function of deposit type-A meta-analysis*, Ore Geol. Rev. 76, 52-78.
- GEORGE, L.L., COOK, N.J., CIOBANU, C.L., 2016. *Partitioning of trace elements in co-crystallized sphalerite-galena-chalcopyrite hydrothermal ores*, Ore Geol. Rev. 77, 97-116.
- HALFYARD, J.E., HAWBOLDT, K., 2011. *Separation of elemental sulfur from hydrometallurgical residue: A review*, Hydrometallurgy 109(1-2), 80-89.
- JANKOLA, W.A., 1995. *Zinc pressure leaching at Cominco*, Hydrometallurgy 39(1), 63-70.

- KASKIALA, T., 2002. *Determination of oxygen solubility in aqueous sulphuric acid media*, Miner. Eng. 15(11), 853-857.
- KRYSA, B.D., 1995. *Zinc pressure leaching at HBMS*, Hydrometallurgy 39(1), 71-77.
- LAMPINEN, M., LARRI, A., TURUNEN, I., 2015. *Kinetic model for direct leaching of zinc sulfide concentrates at high slurry and solute concentration*, Hydrometallurgy 153, 160-169.
- LI, C.X., WEI, C., XU, H.S., DENG, Z.G., LIAO, J.Q., LI, X.B., LI, M.T., 2010. *Kinetics of indium dissolution from sphalerite concentrate in pressure acid leaching*, Hydrometallurgy 105(1-2), 172-175.
- LIANG, D.Q., WANG, J.K., WANG, Y.H., 2009. *Difference in dissolution between germanium and zinc during the oxidative pressure leaching of sphalerite*, Hydrometallurgy 95(1), 5-7.
- MARKUS, H., FUGLEBERG, S., VALTAKARI, D., SALMI, T., MURZIN, D. Y., LAHTINEN, M., 2004. *Reduction of ferric to ferrous with sphalerite concentrate, kinetic modeling*, Hydrometallurgy 73(3-4), 269-282.
- MEYER, B., 1976. *Elemental sulfur*, Chem. Rev. 76(3), 366-388.
- OWUSU, G., 1985. *Interfacial studies in the zinc pressure Leach Technology*, M.Sc. Thesis, University of British Columbia.
- OWUSU, G., DREISINGER, D. B., PETERS, E., 1995. *Interfacial effects of Surface-Active agents under zinc pressure leach conditions*, Metall. Mater. Trans. B, 26(1), 5-12.
- OZBERK, E., JANKOLA, W.A., VECCHIARELLI, M., KRYSA, B.D., 1995. *Commercial operations of the Sherritt zinc pressure leach process*, Hydrometallurgy 39(1-3), 49-52.
- PAPANGELAKIS, V.G., DEMOPOULOS, G.P., 1991. *Acid pressure oxidation of pyrite: reaction kinetics*, Hydrometallurgy 26(3), 309-325.
- RUBISOV, D.H., PAPANGELAKIS, V.G., 1995. *Model-based analysis of pressure oxidation autoclave behavior during process upsets*, Hydrometallurgy 39(1-3), 377-389.
- SCHIMMEL, R.C., FABER, A.J., DE, W.H., BEERKENS, R.G.C., KHOE, G.D., 2001. *Development of germanium gallium sulphide glass fibres for the 1.31  $\mu\text{m}$  praseodymium-doped fibre amplifier*, J. Non-Cryst. Solids 284(1), 188-192.
- TROMANS, D., 1998. *Oxygen solubility modeling in inorganic solutions: concentration, temperature and pressure effects*, Hydrometallurgy 50(5), 279-296.
- TONG, L., DREISINGER, D., 2009a. *The adsorption of sulfur dispersing agents on sulfur and nickel sulfide concentrate surfaces*, Miner. Eng. 22(5), 445-450.
- TONG, L., DREISINGER, D., 2009b. *Interfacial properties of liquid sulfur in the pressure leaching of nickel concentrate*, Miner. Eng. 22(5), 456-461.
- TORRALVO, F.A., FERNANDEZ-PEREIRA, C., 2011. *Recovery of germanium from real fly ash leachates by ion-exchange extraction*, Miner. Eng. 24, 35-41.
- TYSZCZUK, K., KOROLCZUK, M., GRABARCZYK, M., 2007. *Application of gallium film electrode for elimination of copper interference in anodic stripping voltammetry of zinc*, Talanta 71(5), 2098-2101.
- WAN, Q., WANG, T.H., FENG, T., LIU, X.H., LIN, C.L., 2002. *Synthesis of large-area germanium cone-arrays for application in electron field emission*, Appl. Phys. Lett. 81(17), 3281-3283.
- YE, L., COOK, N.J., CIOBANU, C.L., LIU, Y.P., ZHANG, Q., GAO, W., YANG, Y.L., DANYUSHEVSKY, L.V., 2011. *Trace and minor elements in sphalerite from base metal deposits in South China: A LA-ICPMS study*, Ore Geol. Rev. 2011, 39, 188-217.
- ZUO, X.H., 2009. *Zinc sulfide concentrates oxygen pressure leaching two counter-current principle and comprehensive recovery of gallium germanium technology*, Hunan Nonferrous Metals 25, 26-28.